

Synthesis of Silver Nanodendrites on Silicon and Its Application for the Trace Detection of Pyridaben Pesticide Using Surface-Enhanced Raman Spectroscopy

LUONG TRUC QUYNH NGAN,^{1,4,5} KIEU NGOC MINH,¹ DAO TRAN CAO,¹ CAO TUAN ANH,² and LE VAN VU³

1.—Institute of Materials Science, Vietnam Academy of Science and Technology, 18 Hoang Quoc Viet, Hanoi, Vietnam. 2.—Tantrao University, Yenso, Tuyenquang, Vietnam. 3.—Hanoi National University, 334 Nguyen Trai, Hanoi, Vietnam. 4.—e-mail: ltqngan@gmail.com. 5.—e-mail: nganltq@ims.vast.ac.vn

We present the results of the synthesis of arrays of silver nanodendrites (AgNDs) on the surface of a silicon wafer (AgNDs@Si) and the application of them as surface-enhanced Raman scattering (SERS) substrates to detect traces of pesticides, through the example of pyridaben detection. AgNDs were chosen because they contain many of the points that could be considered as “hot spots”, and therefore SERS substrates made from them will have a high Raman enhancement factor. AgNDs were deposited onto the surface of silicon by electrochemical deposition, using an aqueous solution of HF and AgNO₃. The results showed that, after fabrication, a large number of fern-like AgNDs formed on the surface of the silicon. These AgNDs are distributed evenly across the entire silicon surface with a relatively thick density. Pyridaben is a pesticide for the control of mites and some other insects such as white flies, aphids and thrips on fruits, vegetables, tea and ornamentals. Pyridaben is harmful to humans if it is used improperly. When used for the detection of pyridaben, SERS substrates made from fabricated AgNDs@Si were able to detect concentrations as low as 0.1 ppm.

Key words: Silver nanodendrites, electrochemical deposition, surface-enhanced Raman spectroscopy, SERS, pyridaben, pesticide detection

INTRODUCTION

Pesticides are defined as substances or mixtures intended to prevent, destroy, repel or mitigate any pest, including insects, rodents and weeds.¹ Currently, pesticides are being widely used for protecting crops and fruits and play a crucial role in agricultural production. However, with the increase in the number of types and amounts of pesticides employed in agriculture, the threat of pesticide residues to human health is rising. Consequently, the issue of pesticide residues is attracting extensive public attention and merits further investigation.

Pyridaben, whose molecular formula is C₁₉H₂₅ClN₂OS, belongs to a new acaricide pesticide family, the pyridazinones, discovered by Nissan Chemical Industries Ltd. for the control of mites and some other insects, such as white flies, aphids and thrips.² Typically, pyridaben is being developed for application to fruits as a 20% wettable powder, and for vegetables, tea and ornamentals as a 20% suspension concentrate. Although pyridaben has been reported to have low toxicity to mammals, it nonetheless still adversely impacts on their growth and reproduction, especially when used improperly.^{2–4} Therefore, the rapid detection and identification of pyridaben at trace levels is a matter of concern for both users and researchers. At present, the main analytical methods used to identify trace

(Received October 5, 2016; accepted January 1, 2017; published online January 27, 2017)

amounts of pesticides (including pyridaben) are various chromatographic methods, alone or in combination with mass spectrometry, including gas chromatography (GC),^{5–7} high performance liquid chromatography (HPLC)⁸ and liquid chromatography (LC).⁹ Although these methods are effective in determining residues of pesticides in a quantitative way, they still have some limitations such as the requirements of a time-consuming procedure of measurement and sample preparation, as well as the requirement of well-trained laboratory personnel. Therefore, there is a great demand for the development of a simpler, faster and more effective method for the detection of traces of pesticide residues. Concerning the concentration of residues of pyridaben that need to be detected, in 2016 the US Environmental Protection Agency (EPA) established the tolerance of pyridaben residues for fruits at 0.1–3 ppm (depending on the particular fruit).

Raman spectroscopy is a vibrational spectroscopic method that has been recognized as a reliable technique for assessing the safety and quality of food.¹⁰ Raman spectra can provide “fingerprint-like” information for various chemicals and biochemicals with little or no sample preparation. However, traditional Raman spectroscopy is only suitable for detecting high concentrations of the substance to be analyzed, because in normal conditions the probability of Raman scattering is very small.¹¹ Surface-enhanced Raman spectroscopy (SERS) represents a great advance in the field of Raman spectroscopy. SERS is a technique in which molecules adsorbed onto a rough metal surface under certain conditions exhibit an anomalously large interaction cross-section for the Raman effect with the consequence that the Raman signal of these molecules is amplified by several orders of magnitude. With suitable metal nanostructures and measurement setup, SERS can even detect single molecules and achieve a Raman enhancement factor of up to 10^{14} – 10^{15} .^{12,13} Thanks to this great enhancement, along with the advantages of Raman spectroscopy, SERS has become one of the best candidates for the detection of pesticides in food.

At present, it is widely accepted that the high Raman enhancement in SERS is mainly contributed by a huge augmentation of the local electromagnetic (EM) field which originates from the excitation of plasmons on the surface of metals.^{11–14} In general, researchers in the field believe that the intensity of the local EM field can be promoted by two kinds of patterns on the SERS substrates. The first is a sharp tip with high curvature that acts as a ‘lightning rod’ and the second is a gap of nanometer size (also called a nanogap) between neighboring metal nanoparticles or nanostructures. These regions with a greatly enhanced local EM field are often called ‘hot spots’, and they play a decisive role in the enhancement of the Raman signal in SERS. The SERS substrates with multiple hot spots will have a large Raman enhancement. A nanodendrite

is a structure with many hot spots. First, the tips and the sharp edges of the trunk and branches of the dendrite are a kind of hot spots. The second type of hot spots is the narrow gap between the branches. Moreover, because during fabrication we produced not only a nanodendrite but also many piled nanodendrites, one superimposed on the other (which can be called an array of nanodendrites), then the interstices of overlapped branches can also become hot spots. Therefore, the arrays of silver nanodendrites (AgNDs) are expected to show very high SERS activity.

Here, we present the results of the synthesis of arrays of AgNDs on the surface of a silicon wafer (AgNDs@Si) and the application of them as SERS substrates to detect traces of pyridaben pesticide. AgNDs were deposited onto the surface of silicon (Si) by electrochemical deposition, using an aqueous solution of HF and AgNO₃. In a previous work,¹⁴ we have fabricated AgNDs on an Si surface by electroless deposition and electrodeposition (in the constant voltage mode), using the same aqueous solution of AgNO₃ and HF, and then used them as SERS-active substrates to detect trace amounts of paraquat, a commonly used herbicide. The results showed that the electrodeposited AgNDs have much better ramification with a thicker density of the dendrites as well as a better arrangement of dendrites. As a result, the SERS-active substrates made from electrodeposited AgNDs were able to detect paraquat with a detection limit hundreds of times lower than that of the electroless-deposited AgNDs substrates. In this work, we used the constant current mode of electrodeposition to fabricate AgNDs, because the reality has shown that the result of this mode are the dendrites with better branching, compared with that of the constant voltage mode. As for the molecules to be analyzed, to the best of our knowledge, this is the first time that pyridaben has been detected by the means of SERS. In the literature, we have found a few articles that have mentioned the analysis of pyridaben, but by chromatography methods.^{5–9}

EXPERIMENTAL

AgNDs have been electrochemically deposited at room temperature onto the surface of Si, using an aqueous solution of AgNO₃ and HF. The Si used was boron-doped *p*-type single crystalline (100) Si with a resistivity of 0.5–50 Ω cm. The reagents used were of analytical reagent grade with purity as follows: AgNO₃, 99.8%, and HF, 40%. The water used was deionized water. The process of Ag deposition on Si was carried out as follows. First, the Si wafer was cleaned with acetone to remove grease. Next, the clean Si wafer was immersed in 5% HF aqueous solution for 30 min to achieve a H-terminated Si surface. The Si wafer covered by Si–H bonds was then immediately placed into a freshly prepared reduction solution containing 4.8 M of HF and

20 mM of AgNO_3 for 15 min. This deposition condition was chosen because it already gave the Ag dendritic structure during Ag electroless deposition.¹³ The electrodeposition of AgNDs was carried out under the constant current mode using a typical electrodeposition set-up consisting of a constant current power source with a platinum grid used as the anode and the Si wafer used as the cathode. These two electrodes were placed parallel to each other and separated by 2 cm in a Teflon container. Prior to the deposition process, aluminum was evaporated on the back of the Si wafer to create an ohmic contact; this process allowed the Si wafer to be used as an electrode. The deposition process has been performed at a current density value in the range of $1\text{--}3\text{ mA cm}^{-2}$.

The structure and morphology of representative AgNDs@Si samples were examined using a S-4800 field emission scanning electron microscope (SEM; Hitachi, Japan). X-ray diffraction (XRD) analysis was carried out on a Bruker-AXS D5005 diffractometer (Siemens, Germany) using $\text{Cu K}\alpha$ radiation ($k = 0.154056\text{ nm}$). The SERS measurements were performed by dripping $25\ \mu\text{l}$ of pyridaben pesticide solution with different concentrations onto the AgNDs@Si surface. The spreading area is $\sim 0.6 \times 0.6\text{ cm}^2$. Pesticide solutions of different concentrations were prepared using sequential dilution. Pyridaben powder, purchased from Sigma-Aldrich, was dissolved in methanol to prepare a 1000-ppm stock solution. Next, this stock solution was further diluted with deionized water to concentrations for analysis. After pyridaben solution dripping, samples were allowed to stand in air at room temperature until dry. Raman spectra were recorded only when the samples were dried. Raman spectra were recorded with a Raman spectrometer LabRAM HR 800 (HORIBA Jobin-Yvon, France) using a 632.8-nm laser as an excitation source.

RESULTS AND DISCUSSION

The SEM images showing the morphology of the surface of the Si samples after AgNDs deposition in the same solution (containing 20 mM AgNO_3 and 4.8 M HF) for the same time (15 min), but at different current densities (changing from 1 to 3 mA cm^{-2}), are shown in Fig. 1a–c. These images clearly demonstrate that, after the fabrication, a large number of fern-like AgNDs were formed on the surface of the wafer. An Ag dendrite has two- or three-dimensional structures with one long main trunk and short side branches which preferentially grow along two definite directions rather than randomly ramified growth. The short side branches in each branch are parallel to each other and make an angle of about $50^\circ\text{--}60^\circ$ with the trunk, forming symmetric structures. The diameter of the trunks is around 100–150 nm and their length is up to a few dozen micrometers. The length of the branches can also reach tens of micrometers. It is very interesting

that the branches can branch again forming a multi-hierarchical structure. Namely, at the current density of 1 mA cm^{-2} , the ramification includes only 2 levels, as shown in Fig. 1a, but at 2 mA cm^{-2} , some branches had begun to branch out further (branching becoming 3-level), as Fig. 1b demonstrates. At 3 mA cm^{-2} , the majority of the branches already have been further branched, as shown in Fig. 1c. Thus, the branching at 3 mA cm^{-2} is the best, and we have used this current density to produce AgNDs@Si SERS substrates. The above results of good branching also demonstrate the advantages of the constant current mode of silver deposition used in this report, compared with the constant voltage mode used in Ref. ¹⁴. Figure 1d displays the x-ray diffraction (XRD) pattern of AgNDs which has been deposited at 3 mA cm^{-2} onto the Si surface. This figure demonstrates that what has been obtained after electrodeposition was definitively silver, in crystalline form. More specifically, the XRD pattern shows (111), (200) and (220) peaks of the face-centered cubic silver crystal. The strong and sharp diffraction peaks indicate that the Ag dendrites are well crystallized. The intensity of the Ag (111) peak is much stronger than other peaks, indicating that the Ag dendrite growth occurs primarily in the direction of the (111) crystal plane.

The growth mechanism of dendritic structures can be explained using the diffusion-limited aggregation (DLA) model and anisotropic crystal growth.^{14,15} In simple words, the formation process of dendrites can be described as follows. Firstly, Ag nanoparticles (AgNPs) hit and stick with each other forming initial aggregates of AgNPs. Simultaneously, other free nanoparticles will diffuse continually toward the aggregates to form larger aggregates by the continuous hitting and sticking processes. The formation of the AgNPs onto the Si in an aqueous solution containing Ag ions (Ag^+) and HF is based on the reduction of ionic Ag to atomic Ag occur at the Si surface.¹⁴ The AgNPs first arrange themselves in a linear shape forming wire-like and rod-like structures, which will become the dendrite backbones. As the reaction proceeds, the growth is mainly driven by the decreasing surface energy, and the growth of the nanostructure prefers to occur at the tips and stems of the branches. As the stem grows in length, new shorter branches are continuously formed.

To demonstrate that the AgNDs@Si samples can work as highly active SERS substrates, they were used as SERS substrates in detecting traces of pyridaben. For this work, the AgNDs which have been electrodeposited at the current density of 3 mA cm^{-2} were used because, as mentioned above, they have the best ramification. SERS spectra of pyridaben solutions with different pyridaben concentrations dripped on the different AgNDs@Si substrates produced by the same process are shown in Fig. 2. First of all, we can see that the SERS spectrum of pyridaben is complex, with many peaks

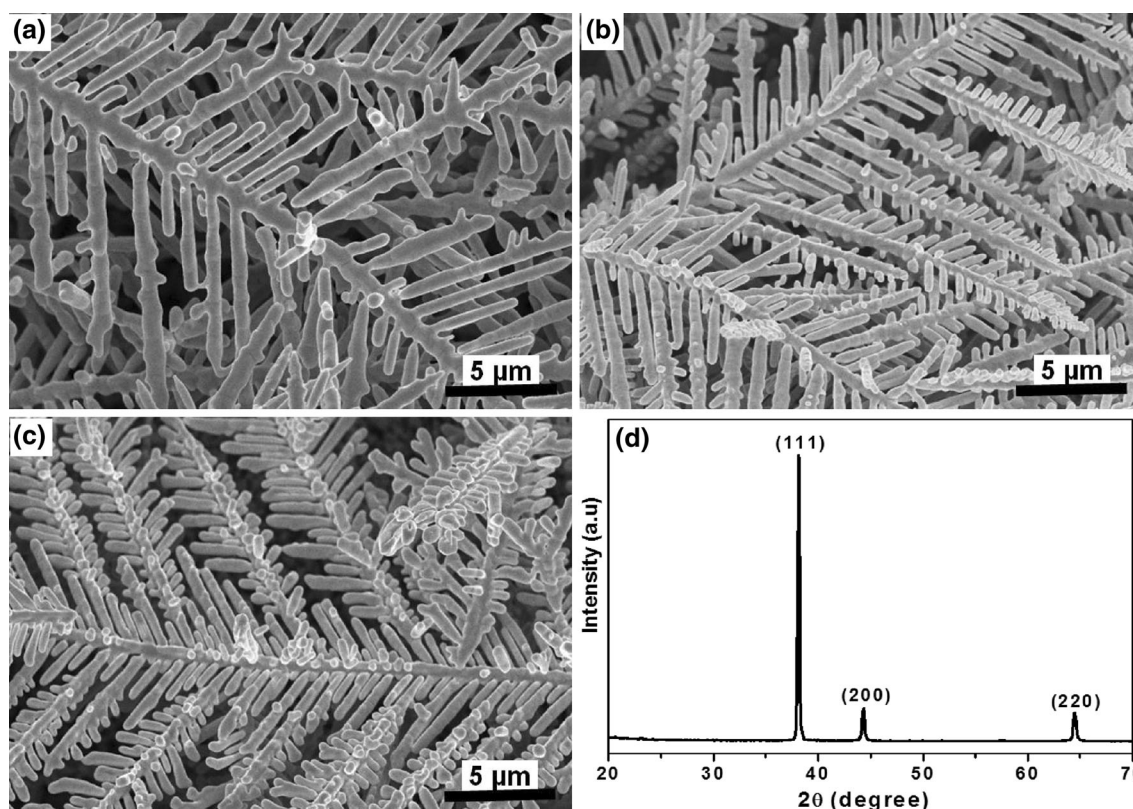


Fig. 1. SEM images of the AgNDs which have been electrodeposited onto Si samples with the current density of 1 mA cm^{-2} (a), 2 mA cm^{-2} (b) and 3 mA cm^{-2} (c), while other conditions are identical: in the aqueous solution of 20 mM AgNO_3 and 4.8 M HF , with the same deposition time of 15 min and XRD pattern of AgNDs which have been electrodeposited onto Si surface at the current density of 3 mA cm^{-2} (d).

distributed throughout the region $600\text{--}1700 \text{ cm}^{-1}$. This is understandable if we recall that the chemical formula of pyridaben is quite complicated ($\text{C}_{19}\text{H}_{25}\text{ClN}_2\text{OS}$). These peaks are associated with vibrations of several groups of their chemical structure, among them C–Cl, C–C, C–H, C–N, C–S, C–O and C=C. Table I summarizes the peak assignments of pyridaben SERS spectra. The most intense peak in the SERS spectra of pyridaben was observed at 635 cm^{-1} and assigned to the ring structure of the molecule. The peaks at 670 cm^{-1} , 811 cm^{-1} , and 1106 cm^{-1} were assigned to the C–Cl stretching mode, while the peaks at 1138 cm^{-1} , 1218 cm^{-1} , and 1482 cm^{-1} are due to the C–N stretching mode. The peaks at 1245 cm^{-1} , 1265 cm^{-1} , and 1280 cm^{-1} were caused by the ring stretching mode and C–H in-plane bending mode, while the peaks at 709 cm^{-1} , and 710 cm^{-1} may be from the C–S stretching mode coupled with C–C–C stretching and C–C in-plane bending mode. Another strong peak at 1648 cm^{-1} can be attributed to the C=O stretching mode, and the peak at 1615 cm^{-1} is assigned to the C=C stretching mode. The bands at 756 cm^{-1} and 780 cm^{-1} are assigned to C–H out-of-plane bending, CH_2 rocking and C–N in-plane bending modes. The peaks observed at 846 cm^{-1} and 944 cm^{-1} were due to the C–H in plane bending

mode, while the peaks at 925 cm^{-1} and 1200 cm^{-1} can be attributed to the CH_3 rocking and CH_2 twisting modes, respectively. These characteristic peaks can be used for qualitative and quantitative analysis of pyridaben molecules.

In Fig. 2, we can clearly see that the intensity of the main peaks of pyridaben dropped steadily when its concentration decreased. This demonstrates that the AgNDs@Si substrates which have been used for the detection of different levels of pyridaben can be regarded as identical. In other words, the process used to manufacture AgNDs on Si is stable and has good repeatability, and the products of this process can be used in the analysis of traces of pyridaben. In addition, we can see from Fig. 2 that, even when the pyridaben concentration in probe solution decreased to 0.1 ppm, we can still observe the characteristic peaks of pyridaben on the SERS spectrum. This proves that, with the fabricated AgNDs@Si substrates, we can identify pyridaben from as low a concentration of 0.1 ppm onwards. Although this threshold value is still higher compared with the threshold value of chromatography methods (for example, in the case of HPLC, the threshold value is 0.01 ppm ⁸), it still meets the safety value of pyridaben as recommended by the US EPA. This result opens up prospects of using Raman spectroscopy to

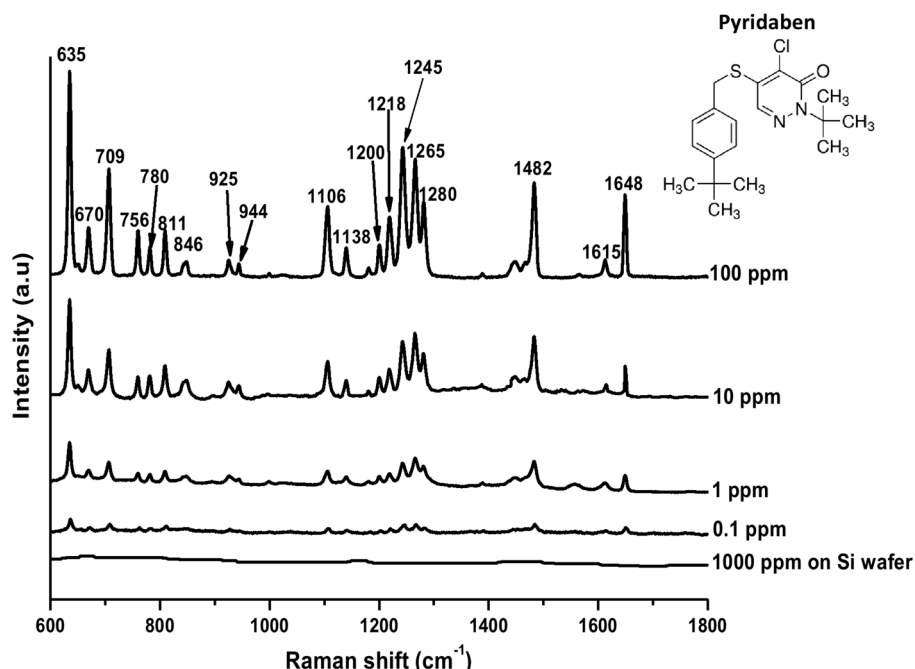


Fig. 2. SERS spectra of pyridaben with different concentrations: 100 ppm, 10 ppm, 1 ppm and 0.1 ppm, which was dripped onto AgNDs@Si substrates fabricated by electrodeposition with the same procedure, and Raman spectra of 1000-ppm stock solution of pyridaben dripped on the flat surface of a Si sample.

Table I. Band assignments of major peaks in Raman spectra of pyridaben

Band (cm ⁻¹)	Assignment	Band (cm ⁻¹)	Assignment
635	δ (ring)	1106	ν (C–Cl); δ (C–H)
670	ν (C–Cl)	1138	ν (C–N); δ (C–H)
709	ν (C–S); ν (C–C–C), δ (C–C)	1200	δ_{tw} (CH ₂); ω (CH ₂)
710	ν (C–S); ν (C–C–C), δ (C–C)	1218	ν (C–N)
756	γ (C–H), ρ (CH ₂), δ (C–N)	1245	ν (ring); δ (C–H)
780	γ (C–H), ρ (CH ₂), δ (C–N)	1265	ν (ring); δ (C–H)
811	ν (C–Cl)	1280	ν (ring); δ (C–H)
846	δ (C–H)	1482	ν (C–N)
925	ρ (CH ₃)	1615	ν (C = C)
944	δ (C–H)	1648	ν (C = O)

ν stretching; δ in-plane bending; γ out-of-plane bending; ρ rocking; δ_{tw} twisting; ω wagging.

determine pyridaben pesticide residues on food as well as in other environments, and thus contribute to the protection of public health.

To confirm the role of AgNDs in the SERS effect, we have dropped a 1000-ppm stock solution of pyridaben onto the Si sample without AgNDs coating and after that performed Raman measurements. The result (also shown in Fig. 2) shows that, without AgNDs, the SERS effect did not occur and we cannot observe characteristic peaks of pyridaben on the obtained Raman spectrum. This result also demonstrates the validity of SERS. Specifically, if the SERS effect does not occur, it will not be able to detect pyridaben by means of traditional Raman spectroscopy, even at high concentrations.

CONCLUSIONS

In summary, using electrochemical deposition of Ag in constant current mode, using a very simple solution of AgNO₃ and HF dissolved and diluted with water, we have succeeded in producing a large number of three-level hierarchical fern-like AgNDs on a Si surface. These AgNDs are distributed evenly across the entire surface of the Si sample, and they have grown up under the overlapping manner, one is overlaid on the other, forming a relatively thick layer of dendrites. Thanks to the fact that there are many tips and sharp edges, as well as a very close distance between the adjacent Ag nanostructures, the AgNDs@Si samples fabricated in such a way can be used as SERS substrates with high Raman

enhancement. To demonstrate this, the fabricated AgNDs@Si samples have been used to detect trace amounts of pyridaben, a pesticide that is often applied to fruits, vegetables, tea and ornamentals, by Raman spectroscopy. The results showed that, with the aforementioned AgNDs@Si SERS substrates, pyridaben may be identifiable in concentrations as low as 0.1 ppm.

ACKNOWLEDGEMENT

This work was supported financially by the Vietnam Academy of Science and Technology (VAST) under project VAST.DLT.04/17-18.

REFERENCES

1. S. Armenta, G. Quintas, S. Garrigues, and M.D.L. Guardia, *Trac-Trend. Anal. Chem.* 24, 772 (2005).
2. E.M. Ghodrat, P. Kazem, H. Shapour, Y. Parichehr, and N. Golamreza, *Comp. Clin. Pathol.* 23, 297 (2014).
3. J.L. Shipp, K. Wang, and G. Ferguson, *Biol. Control* 17, 125 (2000).
4. G.E. Manas, S. Hasanzadeh, and K. Parivar, *Iran. J. Basic. Med. Sci.* 16, 1055 (2013).
5. P. Cabras, A. Angioni, V.L. Garau, M. Melis, F.M. Pirisi, F. Cabitza, F. Dedola, and S. Navickiene, *J. Agric. Food Chem.* 46, 4255 (1998).
6. C. Zhang, H. Zhao, M. Wu, X. Hu, X. Cai, L. Ping, and Z. Li, *J. Chromatogr. Sci.* 50, 940 (2012).
7. Y. Han, F. Dong, J. Xu, X. Liu, Y. Li, Z. Kong, X. Liang, N. Liu, and Y. Zheng, *Food Control* 37, 240 (2014).
8. F. Tian, X. Liu, J. Xu, F. Dong, Y. Zheng, M. Hu, and Y. Wu, *Food Anal. Methods* 9, 2917 (2016).
9. S.W. Kim, A.M. Abdel-Aty, M.M. Rahman, J.H. Choi, O.J. Choi, G.S. Rhee, M.I. Chang, H. Kim, M.D.N. Abid, S.C. Shin, and J.H. Shim, *Biomed. Chromatogr.* 29, 990 (2015).
10. Y.S. Li and J.S. Church, *J. Food Drug Anal.* 22, 29 (2014).
11. T.C. Dao, T.Q.N. Luong, T.A. Cao, N.H. Nguyen, N.M. Kieu, T.T. Luong, and V.V. Le, *Adv. Nat. Sci. Nanosci. Nanotechnol.* 6, 035012 (2015).
12. S. Nie and S.R. Emory, *Science* 275, 1102 (1997).
13. L.T.Q. Ngan, D.T. Cao, C.T. Anh, and L.V. Vu, *Int. J. Nanotechnol.* 12, 358 (2015).
14. T.C. Dao, T.Q.N. Luong, T.A. Cao, N.M. Kieu, and V.V. Le, *Adv. Nat. Sci. Nanosci. Nanotechnol.* 7, 015007 (2016).
15. T.A. Witten and L.M. Sander, *Phys. Rev. B* 27, 5686 (1983).